Biochemical and Biophysical Research Communications 386 (2009) 65–70

Contents lists available at ScienceDirect

Biochemical and Biophysical Research Communications

journal homepage: www.elsevier.com/locate/ybbrc

RGS11 interacts preferentially with R7BP over $G\alpha_{oa}$ – Characterization of Gβ5-free RGS11

Yasar Saleem, Key-Sun Kim *

Center for Neural Science, Korea Institute of Science and Technology (KIST), P.O. Box 131, Cheongryang, Seoul 130-650, Republic of Korea
University of Science and Technology, Daejeon, Republic of Korea

ARTICLE INFO

Article history:
Received 28 May 2009
Available online 2 June 2009

Keywords:
rRGS11
GAP activity
R7BP
SPR
Differential interaction

ABSTRACT

Regulator of G protein signaling 11 (RGS11) is the least characterized member of the R7 family of Gγ-like GGL domain-containing RGS proteins. All R7-RGS proteins of a variety of cell types are found in Gβ5-containing complexes that exhibit a number of unique functional properties. However, presence of Gβ5 reduced the affinity of R7-RGS7 for Gα subunits, also only RGS7 bound to Muscarinic M3-Receptor, but the Gβ5-RGS7 dimer did not, making it difficult to study differential interaction of R7-RGS proteins. Here, we report the successful purification of functionally intact, Gβ5-free recombinant RGS11 (rRGS11), obtained by expressing N- and C-terminally truncated form of RGS11 in *Escherichia coli* BL 21 (DE3), that differentially interact with R7BP and $G\alpha_{oa}$. rRGS11 was capable of interacting with $G\alpha_{oa}$ and R7BP (RGS7 family binding protein) with equilibrium dissociation constants (K_D) of 904 (±208) nM, and 308 (±97) nM, respectively. It also induced several-fold increase in the GTPase activity of $G\alpha_{oa}$. The binding of rRGS11 was differential with a binding preference for R7BP over $G\alpha_{oa}$ implying extended roles of R7BP. In addition, we identified a novel interaction between $G\alpha_{oa}$ and R7BP with a K_D of 592 (±150) nM. The production of stable and functional rRGS11 would provide chances to discover more functions of RGS11 yet to be identified.

Introduction

Regulator of G protein signaling (RGS) proteins enhance intrinsic GTPase activity of the Gα subunit and shortening the lifetime of a given GPCR-mediated signaling event. Thus, RGS proteins in conjunction with GPCR ligands play key roles in GPCR signal transduction. More than 35 different RGS domain-containing proteins, divided into different classes, have been identified to date [1,2].

As with other R7-RGS proteins, including RGS6, RGS7, and RGS9, RGS11 contains an N-terminal Disheveled/EGL-10/Pleckstrin (DEP) domain, a Gγ protein-like (GGL) domain, and a C-terminal RGS domain [3]. The GGL domain of R7-RGS proteins is similar to G protein Gγ subunits, but interacts exclusively with Gβ5. The interaction between R7-RGS proteins and Gβ5 is critical for maintaining mutual stability *in vivo* [4,5]. RGS7 and RGS9 invariably co-purify as tightly associated dimers with Gβ5 and Gβ5L, respectively [6]. However, the RGS7-Gβ5 dimer does not co-precipitate or co-purify with $G\alpha_{oa}$ [7]. The DEP domains of R7-RGS proteins interact with the membrane translocation proteins, R7BP and R9AP (RGS9 anchoring protein) [8,9]. R7BP has been reported to shuttle R7-RGS proteins between the nucleus and the plasma membrane [10], and R9AP is critical for phototransduction regulation and visual perception [9]. However, a recent *in vivo* study revealed that RGS7/Gβ5 is delivered to the dendrites of ON-bipolar cells independently of an association with R7BP [11]. The DEP domain of RGS7 binds to the i3 loop of Muscarinic M3-Receptor (M3R) [12]. The C-terminal RGS domain interacts with Gα subunits and is mainly responsible for GTPase activating protein (GAP) activity toward Gα [3]. Among R7-RGS proteins, RGS11/Gβ5 exhibits the highest GAP activity for $G\alpha_{oa}$ [13]. However, deletion of the DEP domain in RGS11 yields an RGS11ΔD/Gβ5 complex with high GAP activity toward $G\alpha_{oa}$ [3].

RGS11 is expressed mainly in the brain and retina [14,15], and has been studied for its role in controlling μ-opioid receptor (MOR) signaling responses to morphine [16,17]. RGS11 also co-localized with metabotropic glutamate receptor 6 (mGluR6) in retinal ON-bipolar cells [18], suggesting that RGS11 is involved in the mGluR6 signal transduction pathway.

In the recently solved structure of the RGS9-Gβ5 complex [19], RGS9 was shown to wrap around Gβ5. But even with this structural information, differential interactions of Gβ5 with RGS proteins could not be explained. Gβ5 reduced the affinity of R7-RGS7 for Gα subunits [6,7], the full-length RGS7 bound to the i3 loop of M3R, but the Gβ5-RGS7 dimer did not [12] and Gβ5 association does not directly influence the functional architecture of the RGS9-RGS domain [19] rationalizes the possibility of studying R7-RGS in the absence of Gβ5. However, GGL-containing R7-RGS proteins without Gβ5 have been difficult to obtain in large

* Corresponding author. Fax: +82 2 958 6937.
E-mail address: keysun@kist.re.kr (K.-S. Kim).

0006-291X/$ - see front matter © 2009 Published by Elsevier Inc.
doi:10.1016/j.bbrc.2009.05.128

quantities, hampering functional studies of these proteins. This study was therefore designed, first, to evaluate whether RGS11 retains functional properties in the absence of Gβ5; second, to produce recombinant protein usable for in vitro studies of RGS11 for differential interaction with other binding partners; and third, to produce higher yields of functional RGS11 for future structural and biochemical studies.

In this study, we report the successful purification of functionally intact, Gβ5-free, recombinant RGS11 (rRGS11) in *Escherichia* coli BL 21(DE3) and its differential interaction with auxiliary proteins. We also report a novel interaction between $G\alpha_{oa}$ and R7BP.

Materials and methods

Cloning, expression and purification of rRGS11. Different sized variants of RGS11 (GenBank accession no. NM_183337) were cloned into pET-28a and expressed in *E. coli* as inclusion bodies (Supplementary data Table S1). rRGS11 DNA was amplified from RGS11 cDNA (KRIBB, Korea) by PCR using forward (5′-CCGGAATTC ATGCCCGACCAGGGCGTG-3′) and reverse (5′-CCCAAGCTTTTAGTA CATGTCAGACTTCAG-3′) primers, and cloned into pET-28a using *Eco*RI and *Hind*III restriction sites. The recombinant plasmid, pET-28a-rRGS11 was expressed in *E. coli* strain BL21 (DE3) (Novagen, USA). Inoculum was grown at 37 °C in LB media, to an OD_{600} of 0.8 and induced by 1 mM IPTG for 4 h at 37 °C. rRGS11 inclusion bodies were refolded as described by Leal et al. [20] with some modifications. Briefly, inclusion bodies were solubilized in denaturing buffer (50 mM CAPS pH 11.0, 300 mM NaCl, 1% *N*-lauroyl sarcosine) and denatured rRGS11 was purified by Ni-chelating sepharose (Amersham Bioscience, Sweden) following the manufacturer's instructions. Purified fractions were refolded by gradually decreasing the *N*-lauroyl sarcosine and CAPS in dialysis buffer (50 mM Tris–HCl and 150 mM NaCl, pH 11.0), followed by gradual lowering of pH to 7.6. Refolded rRGS11 was again purified using Ni-affinity chromatography and stored in 25 mM HEPES, pH 7.6 with 200 mM NaCl.

CD spectroscopy of rRGS11. Far-UV circular dichroism spectroscopy was used to generate a wavelength scan and analyze the thermal unfolding transition of rRGS11 using a JASCO J-715 spectropolarimeter. Wavelength spectra were recorded from 260–195 nm at 20 °C using a 1-nm nominal bandwidth with six accumulations. A temperature scan from 5–100 °C was performed at a rate of 1 °C/min at 222 nm.

ELISA-based interaction studies. To verify that rRGS11 retained its known ability to associate with $G\alpha_{oa}$ and MBP-R7BP, both proteins were produced in *E. coli* (Supplementary data Fig. S1) and tested for binding. After removing the His_6 tag, rRGS11 was coated onto a high-binding ELISA plate (Corning, USA) by incubating an rRGS11 solution (1 μg/well) overnight at 4 °C. Non-specific binding was blocked by incubating plates with blocking buffer (5% skim milk in PBS, pH 7.4). rRGS11 and His_6-$G\alpha_{oa}$ interactions were determined after first generating a complex of His_6-$G\alpha_{oa}$-GDP-AlF_4^- [21]. Different concentrations of the complex were then incubated with pre-immobilized rRGS11 for 1 h at 23 °C. Bound His_6-$G\alpha_{oa}$ was detected by incubating with His-probe goat monoclonal antibodies (Abcam, USA; diluted 1:1000) for 1 h, and then incubating with HRP-conjugated anti-goat IgG secondary antibodies (Abcam, USA; diluted 1:4000) for 1 h. After every step wells were washed with PBS-T (0.02% triton X-100 in PBS, pH 7.4). The reactions were developed using 1% Immunopure-OPD (Pierce, USA) for 20 min at room temperature and stopped by adding 2 N HCl. The absorbance of triplicate independent experiments was recorded at 490 nm on a Spectramax 340 ELISA plate reader (Molecular Devices, USA). For rRGS11 and MBP-R7BP interaction studies, plates coated with rRGS11 (1.5 μM) were prepared as described above and MBP-R7BP was added. The remaining steps are as described for $G\alpha_{oa}$, except bound MBP-R7BP was detected using MBP-probe rabbit monoclonal antibodies followed by incubation with HRP-conjugated anti-rabbit IgG secondary antibodies.

SPR-based interaction studies. Biomolecular interactions of rRGS11, $G\alpha_{oa}$ and MBP-R7BP were also analyzed by surface plasmon resonance (SPR) using a Biacore 2000 (Biacore, Sweden), a core facility at the Korea Basic Science Institute, Seoul. rRGS11 and $G\alpha_{oa}$ were immobilized on a CM5 biosensor chip (Biacore, Sweden) as

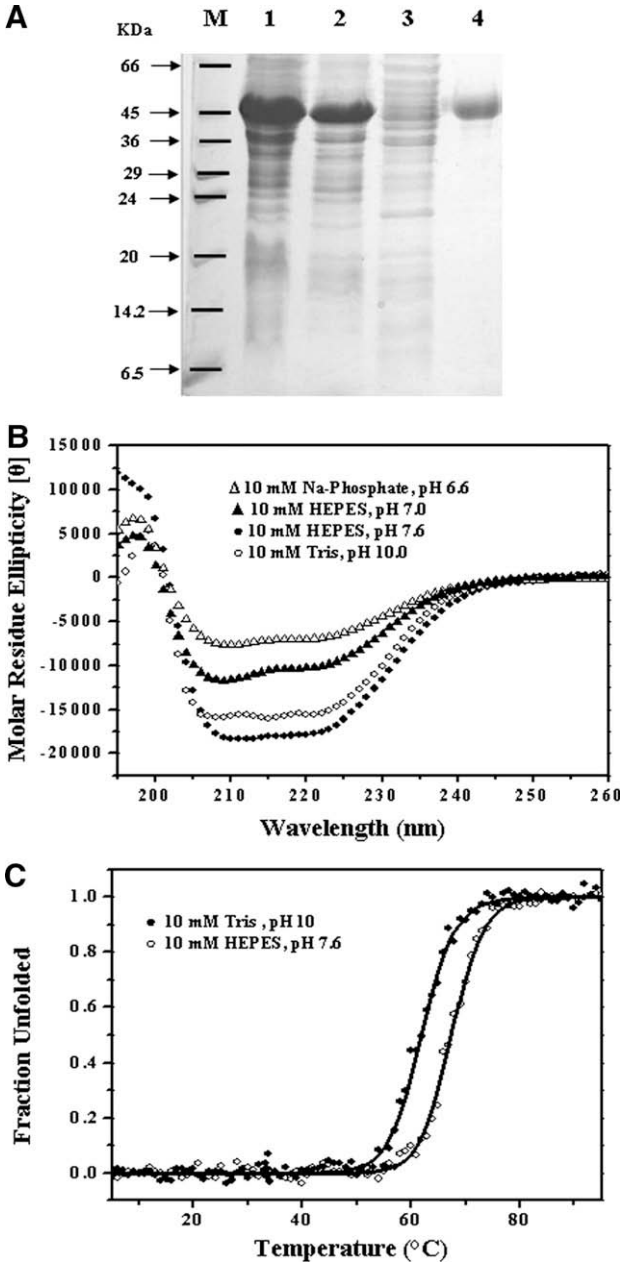

Fig. 1. Purification and CD spectroscopic analysis of rRGS11. (A) Purification of rRGS11 using Ni-affinity resins. M: Molecular-weight marker; 1: whole-cell lysate; 2: pellet; 3: supernatant; 4: final NiNTA eluate refolded and stabilized at pH 7.6. Samples were separated by SDS–PAGE on 15% gels and visualized by Coomassie staining. Marker lines were redrawn to aid visualization. (B) Far-UV wavelength scan (260-195 nm) of rRGS11 at different pHs (theoretical pI 8.75) by CD at 20 °C. Mean values of six accumulations were plotted. The corresponding buffer blanks were subtracted from the data before plotting molar residue ellipticity. (C) Thermal denaturation analysis of rRGS11 at specified pH using CD. Thermal denaturation at different pH with corresponding simulated data (solid lines) is plotted. Data was fit to the Vant Hoff's equation.

described by the manufacturer. Briefly, after chip activation with 0.1 M of NHS and 0.4 M of EDC, rRGS11 or $G\alpha_{oa}$ (both in 10 mM sodium acetate buffer pH 4.0) were passed through the flow cells. rRGS11 was immobilized to a final 1500 resonance units (RU), while $G\alpha_{oa}$ was immobilized to a final of either 800 RU (for kinetic analysis) or 5000 RU (for multianalyte binding experiments), followed by capping the sensor chip with1 M ethanolamine (pH 8.5). The kinetics of binding were determined as described previously by Soundararajan et al. [22], by injecting a series of samples with different protein concentrations for a specified time, followed by injection of an eluent buffer (25 mM HEPES, pH 7.4, 150 mM NaCl) at 25 °C. The chip surfaces were regenerated by 0.05% SDS in 25 mM HEPES (pH 8.0). Kinetic parameters were determined using Biaevaluation 3.1 (Biacore, Sweden). Multiple analyte binding experiments were performed by programmed run of different analytes as described previously by Homola et al. [23]. All binding curves were corrected for background and bulk refractive index contribution by subtraction of the reference flow cells.

GTPase assay. Single-turnover GTPase assays were performed as described previously by Snow et al. [3] and Berman et al. [24]. Briefly, $G\alpha_{oa}$ was first incubated with [γ-^{32}P]GTP (1 μM; Amersham, USA) for 15 min at 20 °C in GTPase buffer (50 mM HEPES pH 7.4, 1 mM DTT, 5 μg/ml BSA), and the reaction was chilled on ice to obtain the [γ-^{32}P]GTP-$G\alpha_{oa}$ complex. The binding of [γ-^{32}P]GTP with $G\alpha_{oa}$ was confirmed using a standard nitrocellulose filter paper binding assay. The reaction was initiated by adding [γ-^{32}P]GTP-$G\alpha_{oa}$ complex (200 nM) to rRGS11 (2 μM) in assay buffer with 1 mM cold GTP and 3 mM $MgCl_2$ (final volume: 50 μl) at 4 °C, and stopped by 5% charcoal slurry in 50 mM phosphoric acid (pH 3.0) and measured radiolabeled inorganic phosphate released into the supernatant using a Packard liquid scintillation analyzer. The reaction rate was calculated for catalyzed and un-catalyzed reactions after 5 min. Raw cpm values were converted into a molar ratio using an online Graphpad Radioactivity Calculator (http://graphpad.com/quickcalcs/radcalcform.cfm). The experiments were repeated three times.

Results and discussion

Production, refolding and CD spectroscopy of rRGS11

RGS11 is known to exist as a complex with Gβ5. Despite the importance of Gβ5 in regulating intracellular expression and stability of RGS11, it is not known whether RGS11, if expressed alone, would be stable and functional. We have addressed this question in the current study, showing that RGS11 retains in vitro activity in the absence of Gβ5, and further, we investigated rRGS11 interaction with other proteins in quantitative terms. We also studied differential interaction of rRGS11 with auxiliary proteins.

To characterize RGS11 in isolation from its potential binding partners, we designed variable-length RGS11 constructs and tested expression and refolding potentials of *E. coli-expressed* proteins. Most truncated protein variants did not express well or fold properly. The lone exception was RGS11 [P^{32}–Y^{414}], designated rRGS11, which was expressed in inclusion bodies and was refolded by dissolving rRGS11 inclusion bodies in 1% (w/v) *N*-lauroyl sarcosine in 50 mM CAPS (pH 11.0) (Supplementary data Figs. S2 and S3; Table S1). The gradual dilution of denaturing agents and subsequent pH reduction produced a protein that was completely soluble up to 0.8 mg/mL. Protein yield after refolding was estimated to be 8 mg/L of culture broth, and purity was greater than 95% (Fig. 1A). Previously 75 μg/L of RGS11/Gβ5 could be produced by Hooks et al. [13].

To evaluate the structural integrity of the refolded protein, we analyzed rRGS11 conformation by CD spectroscopy. The far-UV CD spectrum showed that rRGS11 protein retained a well-folded structure at pH 7.6; but became destabilized at more alkaline or acidic conditions (Fig. 1B). The pH-dependence of rRGS11 structure suggested that most charged residues were involved in electrostatic interactions contributing to protein stability. As with RGS9, which is a helical protein [19], the structure of rRGS11 inferred from CD spectroscopy had a high helix content. However, based on the reported structure of the RGS9/Gβ5 complex, Gβ5 organizes the domains by wrapping around them [19]. Each domain of RGS11

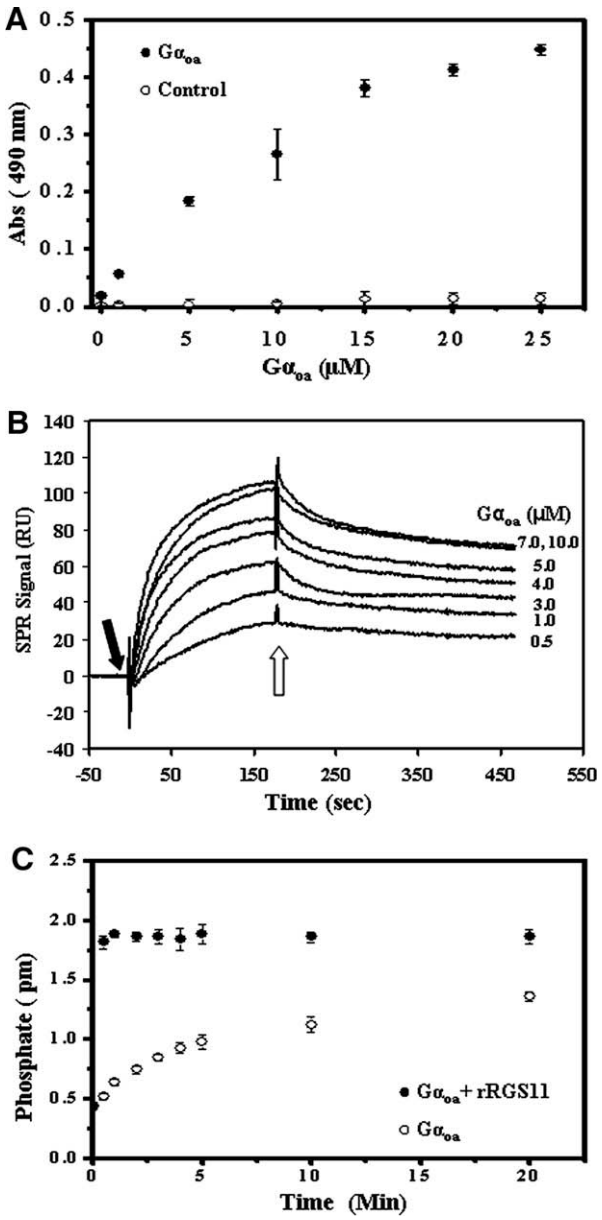

Fig. 2. Interaction analysis of rRGS11 with $G\alpha_{oa}$ and GAP effect of rRGS11. (A) rRGS11 and $G\alpha_{oa}$ interaction determined by ELISA. rRGS11 and $G\alpha_{oa}$ interacted in a concentration-dependent manner. BSA (1 μg/ml)-coated plates were used as a negative control. (B) SPR sensorgram of rRGS11 binding to $G\alpha_{oa}$. One representative sensorgram demonstrating concentration-dependent binding of $G\alpha_{oa}$ to rRGS11 is shown. The black arrow indicates the start of injection of different concentrations of $G\alpha_{oa}$ (association phase), and the white arrow indicates the start of injection of eluent buffer (dissociation phase). ($G\alpha_{oa}$ denotes $G\alpha_{oa}$-GDP-AlF_4^-). (C) [γ-^{32}P]GTP-$G\alpha_{oa}$ (200 nM) was used as the substrate for rRGS11 (2 μM) in a single-turnover GAP assay performed at 4 °C. Released $^{32}P_i$ was monitored after the addition of Mg^{2+} to initiate the reaction. The intrinsic GTPase activity of $G\alpha_{oa}$ and the accelerating effect of rRGS11 on GTPase activity of $G\alpha_{oa}$ is shown. Data are presented as the mean ± SD of triplicate determinations.

Table 1
Kinetic parameters obtained from mutual interaction of rRGS11, $G\alpha_{oa}$ and R7BP by SPR.

Ligand	Analyte	K_a ($M^{-1}s^{-1}$)	K_d (s^{-1})	K_D (Mean ± SD) nM	X^2
rRGS11 (1500 RU)	$G\alpha_{oa}$	3.68×10^3	4.16×10^{-3}	1130 (904 ± 208, $n = 4$)	4.71
rRGS11 (1500 RU)	R7BP	6.16×10^3	2.75×10^{-3}	446 (308 ± 97, $n = 5$)	1.86
$G\alpha_{oa}$ (800 RU)	R7BP	7.98×10^3	4.05×10^{-3}	507 (592 ± 150, $n = 4$)	9.57

k_a, observed kinetic association rate constant; k_d, observed kinetic dissociation rate constant and $K_D = k_d/k_a$, equilibrium dissociation constant. The K_a, K_d and K_d values are calculated from sensorgrams according to Biaevaluation 3.1 manual.
The values are from one representative data set, except Mean ± SD obtained from corresponding '*n*' independent experiments.

and RGS9 has independent functions and, without Gβ5, might move independently.

Protein structure integrity was also evaluated by thermal unfolding analysis. These experiments showed that the unfolding transition temperature (*Tm*) at pH 7.6 was 68 °C compared to a *Tm* of 62 °C at pH 10.0, confirming that rRGS11 was much more stable at pH 7.6 than at pH 10.0 (Fig. 1C).

Analysis of rRGS11 and $G\alpha_{oa}$ interaction by ELISA and SPR

Using ELISA to measure the affinity of rRGS11 for $G\alpha_{oa}$, we found that the proteins interacted in a concentration-dependent manner (Fig. 2A). We confirmed these observations using SPR, which is a powerful tool for real-time measurement of direct protein–protein interactions. A representative sensorgram (Fig. 2B) depicts a resonance response indicative of a concentration-dependent interaction between rRGS11 and $G\alpha_{oa}$. A kinetic analysis of SPR data using Biaevaluation software yielded equilibrium dissociation constant (K_D) = 904 ± 208 nM ($n = 4$) (Table 1).

GTPase assay

We also verified that RGS11 retained the predicted GAP activity toward $G\alpha_{oa}$. Single turnover GTPase assay [3,24] showed that rRGS11 enhanced the GTPase activity of $G\alpha_{oa}$ ~8-fold (from 0.18/min to 1.43/min). The earliest time point we could measure under our assay conditions was 30 s, at which point GTPase activity in the presence of added rRGS11 was maximally enhanced (Fig. 2C). This GAP activity level is consistent with a study by Snow and colleagues [3], who reported approximately a 25-fold enhancement of GTPase activity by an RGS11ΔD/Gβ5 complex. This difference in activation and inhibition might be because of between-study differences in constructs, purification procedures, and/or assay conditions.

Analysis of rRGS11 and MBP-R7BP interaction by ELISA and SPR

As a further validation of the functional properties of rRGS11, we tested rRGS11 ability to bind R7BP. The affinity of rRGS11 for MBP-R7BP was first measured by ELISA (Fig. 3A). We further investigated the kinetics of rRGS11 and MBP-R7BP binding by SPR, indicating K_D = 308 ± 97 nM ($n = 5$) (Table 1, Fig. 3B).

Analysis of $G\alpha_{oa}$ and MBP-R7BP interaction by SPR

We observed novel interaction between $G\alpha_{oa}$ and R7BP. The affinity of $G\alpha_{oa}$ for MBP-R7BP was first analyzed by ELISA, GPC and CD (data not shown). After we got clear evidence that both proteins have binding affinity with each other, we further investigated the binding kinetics of $G\alpha_{oa}$ and MBP-R7BP by SPR and obtained K_D = 592 (±150) nM ($n = 4$) (Table 1, Fig. 4A). These results are consistent with the observation of Cao and colleagues; they also reported co-localization of R7BP and $G\alpha_o$ in retina [11].

Differential binding of rRGS11 and MBP-R7BP with $G\alpha_{oa}$ ligand

Further, we characterized differential binding of rRGS11, MBP-R7BP and $G\alpha_{oa}$ by multiple analyte binding experiments, using $G\alpha_{oa}$ as ligand and injecting rRGS11 and MBP-R7BP. It was observed that rRGS11 (3 μM), in the absence GDP-AlF_4^-, has low binding affinity with $G\alpha_{oa}$ while MBP-R7BP (3 μM) under same conditions bind to $G\alpha_{oa}$ ligand very strongly. Interestingly rRGS11 and MBP-R7BP (1:1 complex, 3 μM each) also has low binding affinity with $G\alpha_{oa}$ (Fig. 4B). Binding affinity doesn't change by

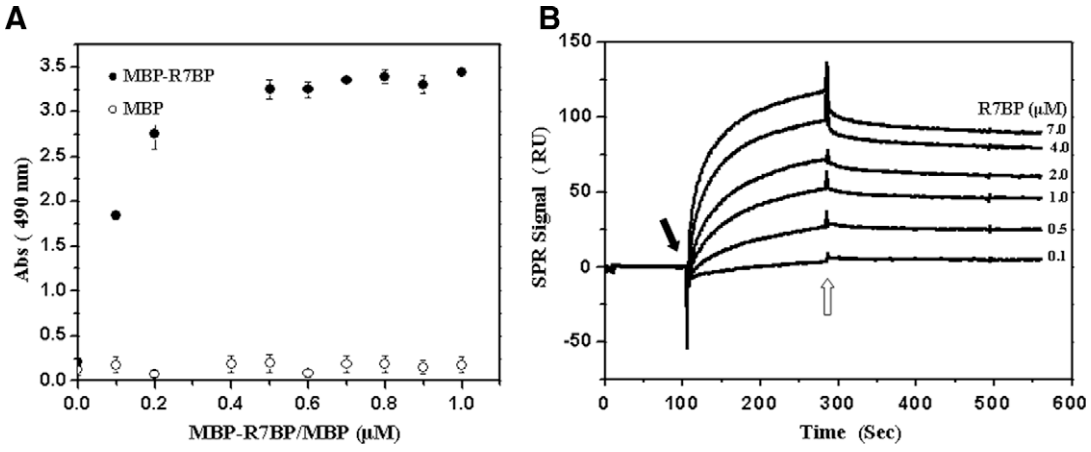

Fig. 3. Interaction analysis of rRGS11 with MBP-R7BP. (A) rRGS11 and MBP-R7BP interaction determined by ELISA. Plot of rRGS11 and MBP-R7BP binding curve is shown, MBP-only control experiment performed in parallel. (B) SPR sensorgram of rRGS11 binding to MBP-R7BP. One representative sensorgram of rRGS11 binding to MBP-R7BP is shown. The black arrow indicates the start of injection of MBP-R7BP and the white arrow indicates the start of injection of buffer.

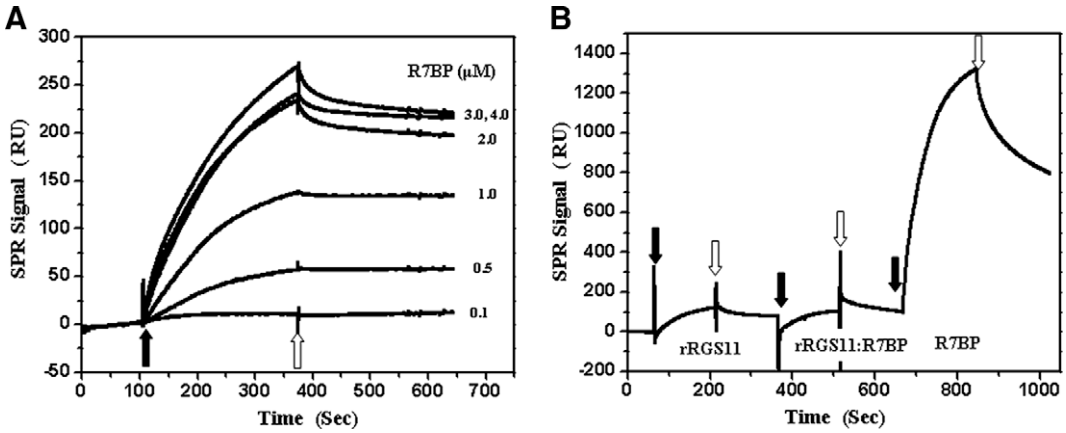

Fig. 4. Interaction analysis of $G\alpha_{oa}$ with MBP-R7BP and differential interaction of rRGS11, MBP-R7BP and $G\alpha_{oa}$ (A) Representative kinetic binding senorgram of $G\alpha_{oa}$ to R7BP is shown here, the concentration dependence of R7BP on binding affinities with $G\alpha_{oa}$ is evident. The black arrow indicates the start of injection of different concentrations of MBP-R7BP and white arrow indicates the start of injection of buffer alone. (B) Representative of three independent multiple analyte binding senorgrams of immobilized $G\alpha_{oa}$ to rRGS11 (3 μM, first analyte sample), rRGS11: MBP-R7BP (1:1, 3 μM each, second analyte sample) and MBP-R7BP (3 μM, third analyte sample) is shown here. The black arrows indicate the start of injection of analytes and white arrows indicate the start of injection of buffer alone. Only MBP-R7BP individually binds with $G\alpha_{oa}$, the complex containing same amount of MBP-R7BP has very low binding affinity with $G\alpha_{oa}$.

different order of injecting the analytes (Supplementary data Fig. S4). This signifies that although same amount of R7BP is present in complex but it remains in complex with rRGS11 and doesn't make a complex with $G\alpha_{oa}$ ligand. Only free R7BP, which is not in complex with RGS11, binds to ligand. This fact was confirmed by injecting complexes of rRGS11 and MBP-R7BP with varying concentrations of both components (Supplementary data Fig. S5). In these experiments, binding was performed in the absence GDP-AlF_4^- to highlight the point that R7BP binds to $G\alpha_{oa}$ in a non-GTPase manner. Lower affinity of rRGS11 with $G\alpha_{oa,}$ in this experiment, compared to that of Fig. 2, is due to the absence of transition state like complex of $G\alpha_{oa}$ (with GDP-AlF_4^-) which is used to analyze binding with RGS proteins (Fig. 2 and Ref. [21]).

To the nest of our knowledge, this is the first reported characterization of RGS11 without Gβ5, and includes an analysis of the binding kinetics of rRGS11 with $G\alpha_{oa}$ and R7BP. Here we are reporting novel $G\alpha_{oa}$ and R7BP interaction also differential binding of rRGS11 with $G\alpha_{oa}$ and R7BP. In summary, we cloned and purified rRGS11 from *E. coli* inclusion bodies. The refolded rRGS11 was stable and retained all known biochemical functions of RGS11/Gβ5 complexes. $G\alpha_{oa}$ directly interacts with R7BP while, rRGS11 differentially interacts with $G\alpha_{oa}$ and R7BP, the reasons for this difference are not yet known.

Acknowledgments

The authors especially wish to thank Prof. Y.G. Yu and Dr. V.K. Moorthy, Kookmin University, for providing the $G\alpha_{oa}$-pET28a clone and critically reading the manuscript; Prof. K.Y. Hwang and A. Priydarshi, Korea University, for helping with the purification of MBP-R7BP; Dr. H.W. Rhim, KIST, for providing the rat brain cDNA library; Dr. M.H. Nam, Korea Basic Science Institute, Seoul, for her help with SPR experiments; and Ms. S.L. Farrar for English editing of the manuscript. The research work was supported by a Korea Research Fund grant funding the Ph.D. work of Y.S. under the supervision of K-S. K.

Appendix A. Supplementary data

Supplementary data associated with this article can be found, in the online version, at doi:10.1016/j.bbrc.2009.05.128.

References

[1] M.B. Jones, D.P. Siderovski, S.B. Hooks, The Gβγ dimer as a novel source of selectivity in G-protein signaling: GGL-ing at convention, Mol. Interv. 4 (2004) 200–214.
[2] G.B. Willars, Mammalian RGS proteins: multifunctional regulators of cellular signalling, Semin.Cell Dev. Biol. 17 (2006) 363–376.
[3] B.E. Snow, A.M. Krumins, G.M. Brothers, et al., A G protein gamma subunit-like domain shared between RGS11 and other RGS proteins specifies binding to Gβ5 subunits, Proc. Natl. Acad. Sci. USA 95 (1998) 13307–13312.
[4] C.-K. Chen, P. Eversole-Cire, H. Zhang, et al., Instability of GGL domain-containing RGS proteins in mice lacking the G protein β-subunit Gβ5, Proc. Natl. Acad. Sci. USA 100 (2003) 6604–6609.
[5] J.Y. Zhou, P.T. Toth, R.J. Miller, Direct interactions between the heterotrimeric G protein subunit Gβ5 and the G protein γ subunit-like domain-containing regulator of G protein signaling 11: gain of function of cyan fluorescent protein-tagged Gγ3, J. Pharmacol. Exp. Ther. 305 (2003) 460–466.
[6] D.S. Witherow, Q. Wang, K. Levay, J.L. Cabrera, et al., Complexes of the G protein subunit Gβ5 with the regulators of G protein signaling RGS7 and RGS9. Characterization in native tissues and in transfected cells, J. Biol. Chem. 275 (2000) 24872–24880.
[7] K. Levay, J.L. Cabrera, D.K. Satpaev, et al., Gβ5 prevents the RGS7-Gαo interaction through binding to a distinct Gγ-like domain found in RGS7 and other RGS proteins, Proc. Natl. Acad. Sci. USA 96 (1999) 2503–2507.
[8] K.A. Martemyanov, P.J. Yoo, N.P. Skiba, et al., R7BP, a novel neuronal protein interacting with RGS proteins of the R7 family, J. Biol. Chem. 280 (2005) 5133–5136.
[9] M. Jayaraman, H. Zhou, L. Jia, et al., R9AP and R7BP: traffic cops for the RGS7 family in phototransduction and neuronal GPCR signaling, Trends Pharmacol. Sci. 30 (2009) 17–24.
[10] R.M. Drenan, C.A. Doupnik, M.P. Boyle, et al., Palmitoylation regulates plasma membrane-nuclear shuttling of R7BP, a novel membrane anchor for the RGS7 family, J. Cell Biol. 169 (2005) 623–633.
[11] Y. Cao, H. Song, H. Okawa, et al., Targeting of RGS7/Gβ5 to the dendritic tips of ON-bipolar cells is independent of its association with membrane anchor R7BP, J. Neurosci. 28 (2008) 10443–10449.
[12] S.L. Sandiford, V.Z. Slepak, The Gβ5-RGS7 complex selectively inhibits muscarinic M3 receptor signaling via the interaction between the third intracellular loop of the receptor and the DEP domain of RGS7, Biochemistry 48 (2009) 2282–2289.
[13] S.B. Hooks, G.L. Waldo, J. Corbitt, et al., RGS6, RGS7, RGS9, and RGS11 stimulate GTPase activity of Gi family G-proteins with differential selectivity and maximal activity, J. Biol. Chem. 278 (2003) 10087–10093.
[14] C. Larminie, P. Murdock, J.-P. Walhin, et al., Selective expression of regulators of G-protein signaling (RGS) in the human central nervous system, Mol. Brain Res. 122 (2004) 24–34.
[15] J.H. Song, H. Song, T.G. Wensel, et al., Localization and differential interaction of R7 RGS proteins with their membrane anchors R7BP and R9AP in neurons of vertebrate retina, Mol. Cell. Neurosci. 35 (2007) 311–319.
[16] J. Garzon, M. Rodriguez-Munoz, A. Lopez-Fando, et al., Activation of μ-opioid receptors transfers control of Gα subunits to the regulator of G-protein signaling RGS9–2: role in receptor desensitization, J. Biol. Chem. 280 (2005) 8951–8960.

[17] A. Lopez-Fando, M. Rodriguez-Munoz, P. Sanchez-Blazquez, et al., Expression of neural RGS-R7 and Gβ5 proteins in response to acute and chronic morphine, Neuropsychopharmacology 30 (2004) 99–110.
[18] C.W. Morgans, T.G. Wensel, R.L. Brown, et al., Gβ5-RGS complexes co-localize with mGluR6 in retinal ON-bipolar cells, Eur. J. Neurosci. 26 (2007) 2899–2905.
[19] M.L. Cheever, J.T. Snyder, S. Gershburg, et al., Crystal structure of the multifunctional Gβ5-RGS9 complex, Nat. Struct. Mol. Biol. 15 (2008) 155–162.
[20] A.T. Leal, P.C. Pohl, C.A.S. Ferreira, et al., Purification and antigenicity of two recombinant forms of Boophilus microplus yolk pro-cathepsin expressed in inclusion bodies, Protein Expr. Purif. 45 (2006) 107–114.
[21] F.S. Willard, A.J. Kimple, C.A. Johnston, et al., A direct fluorescence-based assay for RGS domain GTPase accelerating activity, Anal. Biochem. 340 (2005) 341–351.
[22] M. Soundararajan, F.S. Willard, A.J. Kimple, et al., Structural diversity in the RGS domain and its interaction with heterotrimeric G protein α-subunits, Proc. Natl. Acad. Sci. USA 105 (2008) 6457–6462.
[23] J. Homola, H. Vaisocherová, J. Dostálek, et al., Multi-analyte surface plasmon resonance biosensing, Methods 37 (2005) 26–36.
[24] D.M. Berman, T.M. Wilkie, A.G. Gilman, GAIP and RGS4 are GTPase-activating proteins for the Gi subfamily of G protein α subunits, Cell 86 (1996) 445–452.